JOINT INSTITUTE FOR NUCLEAR RESEARCH
Flerov Laboratory for Nuclear Reaction

FINAL REPORT ON THE START PROGRAMME

MICROMECHANICAL TESTING OF REACTOR MATERIALS IN THE INITIAL STATE AND AFTER IRRADIATION

Supervisor:

Dr. V. A. Skuratov

Student:

Gulnisa V. Tarverdiyeva,

Republic of Kazakhstan,

Al-Farabi Kazakh National University

Participation period:
February 15 – March 28,
Winter Session 2026
Dubna, 2026

CONTENTS

Abstract

In this work, the effect of helium and hydrogen ion implantation on the mechanical properties of austenitic stainless steels 304L and 316L was investigated. In addition, pre-irradiation processing of the high-entropy alloy CoCrFeNiMn was performed. The samples were irradiated with 3 MeV He and 1 MeV H ions, resulting in the formation of a subsurface layer with a relatively uniform distribution of implanted gases. Post-irradiation annealing at 550 °C and 650 °C was carried out to promote diffusion processes and the evolution of gas-filled defects. The mechanical properties were evaluated by nanoindentation. It was shown that irradiation leads to an increase in hardness, while subsequent annealing results in its decrease, which is associated with changes in the defect structure. The contribution of radiation-induced defects to hardening was analyzed within the framework of the dispersed barrier hardening (DBH) model.

1. Introduction

The development of radiation-resistant structural materials for nuclear power plants is one of the key tasks of modern materials science. The efficiency and safety of nuclear reactors strongly depend on the ability of materials to retain their properties under intense irradiation. Materials in the reactor core, including fuel cladding, structural elements and internal components, operate at high temperatures, significant mechanical loads and under the influence of high-energy neutron fluxes. Under these conditions, radiation defects accumulate, leading to changes in the microstructure and degradation of the mechanical properties of materials [1,2].

One of the most significant factors of radiation damage to structural materials is the formation and accumulation of gaseous transmutation products, primarily helium and hydrogen. Helium is produced as a result of (n,α)-reactions and is characterized by extremely low solubility in metallic matrices. Consequently, helium atoms are effectively trapped by crystal lattice defects, such as vacancies, dislocations and grain boundaries, where they form stable complexes and gas-filled bubbles. The growth of such bubbles, in turn, leads to material swelling, reduced ductility and the development of high-temperature embrittlement [3]. Hydrogen also actively interacts with the defect structure, forming complexes with vacancies and other defects. Unlike helium, its effect is more complex: hydrogen can both stabilize vacancy clusters and increase the mobility of point

defects, promoting their recombination. The simultaneous presence of helium and hydrogen can significantly alter the kinetics of defect processes, affecting the evolution of the microstructure and mechanical properties of materials under irradiation.

The most reliable data on the behavior of materials under nuclear reactor operating conditions can be obtained during neutron irradiation tests. However, such experiments are characterized by a significant irradiation duration, which can last several years, and also require complex and expensive post-irradiation processing and analysis of samples. These circumstances significantly limit the possibilities for systematic investigation of radiation effects. In this regard, accelerator-based methods for simulating radiation damage are widely used in radiation materials science. Ion irradiation using accelerators makes it possible to reproduce the main mechanisms of radiation defect formation in a significantly shorter time and provides a high level of control over experimental parameters, including ion type, energy, irradiation temperature and fluence [4-6].

Despite these advantages, ion irradiation has important limitations. In particular, it produces a highly non-uniform concentration and damage profiles with a peak near the end of the ion range, while the thickness of the damaged layer is limited to a few micrometers (Fig.1).

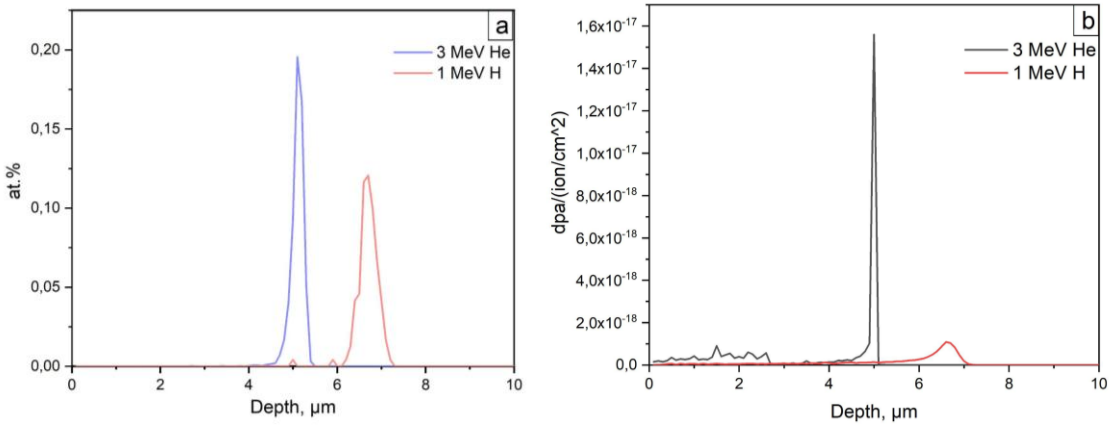

Fig. 1. Concentration (a) and damage profiles (b) calculated using SRIM for the Cantor alloy irradiated with 3 MeV He and 1 MeV H ions.

The small thickness of the irradiated layer significantly limits the application of traditional mechanical testing methods, such as tensile or bending tests of macroscopic samples. To study mechanical properties under such conditions, alternative mechanical testing methods are widely used, in particular

nanoindentation [7]. This method makes it possible to determine the mechanical characteristics of a material at shallow depths and is widely used to study radiation hardening in ion-irradiated materials [8,9]. In addition to standard indentation tests, nanoindentation can be combined with microsample methods fabricated using a focused ion beam (FIB), which allows tensile, bending and other types of loading tests on microscale samples [10].

An important condition for the correct application of the nanoindentation method is the homogeneity of the studied material layer, which is especially important in the case of studying ion-irradiated samples. To solve this problem, special irradiation techniques can be used to form a layer with a nearly uniform concentration of implanted gases at a given depth. Thus, in the present work, irradiation was carried out using the homogeneous implantation method [11], which ensures the formation of an extended layer with an almost constant concentration of the impurity gas.

The aim of this work is to investigate the effect of helium and hydrogen ion implantation on the mechanical properties of model austenitic steels 304L and 316L after subsequent thermal annealing, which stimulates the evolution of the defect microstructure and the growth of gas bubbles. The obtained results are compared with literature data on the parameters of the radiation-induced microstructure and the mechanisms of radiation hardening. In addition, pre-irradiation preparation of the high-entropy alloy CoCrFeNiMn was carried out for subsequent studies of its radiation resistance.

2. Literature Review

2.1. Ion irradiation as a method for simulating reactor damage

Direct studies of materials under nuclear reactor conditions are associated with significant challenges, including long irradiation times, high cost, and the complexity of post-irradiation examination. Therefore, accelerator-based ion irradiation methods are widely used to simulate radiation damage. In these methods, material damage is produced by energetic ions, which lose energy through both elastic collisions with atomic nuclei (nuclear stopping) and inelastic interactions with electrons (electronic stopping). As a result, atoms are displaced from their lattice sites, forming displacement cascades that reproduce the primary damage state caused by fast neutrons.

In some accelerator systems, irradiation is performed in a pulsed beam mode, which can influence the kinetics of radiation-induced processes [4]. During

the intervals between pulses, partial relaxation of radiation defects may occur, including recombination, migration, and annihilation. This can lead to differences in defect accumulation compared to continuous irradiation conditions typical of nuclear reactors. In particular, both experimental and modeling studies indicate that pulsed irradiation may reduce defect accumulation rates and affect processes such as radiation swelling, especially at intermediate temperatures. The magnitude of this effect depends on the pulse frequency relative to characteristic defect migration times. Another important feature of ion irradiation is the limited thickness and non-uniformity of the damage profile. As ions penetrate the material, they gradually lose energy and come to rest at a certain depth. This results in the formation of a pronounced damage peak (Bragg peak) near the end of the ion range, typically located at depths from tens of nanometers to several micrometers depending on the ion type and energy. Such inhomogeneity complicates the analysis of mechanical properties, since conventional testing methods probe a volume that includes both irradiated and unirradiated material.

2.2. The problem of gas accumulation in structural materials

One of the key factors in the degradation of structural materials under irradiation is the accumulation of gaseous transmutation products, primarily helium and hydrogen. Under reactor conditions, these gases are generated through nuclear reactions. Due to their low solubility in metallic matrices, helium atoms are efficiently trapped by point defects, particularly vacancies, forming stable He–vacancy complexes and clusters. They also interact with extended defects such as voids, dislocations, and grain boundaries [12-14]. With increasing temperature, defect migration and coalescence processes become more active, leading to the growth of bubbles. The formation and evolution of such bubbles are among the primary causes of radiation swelling and high-temperature embrittlement. Therefore, understanding the mechanisms of helium accumulation and evolution is essential for predicting the lifetime of structural materials under reactor conditions.

In the case of ion irradiation, an important factor is the spatial distribution of implanted gas atoms. It is well known that conventional ion irradiation produces highly non-uniform profiles of both damage and implanted species. Several approaches have been proposed to obtain a more uniform distribution with depth. One such approach is the use of a wheel degrader, which allows multiple implantation peaks to be superimposed along the depth [15,16].

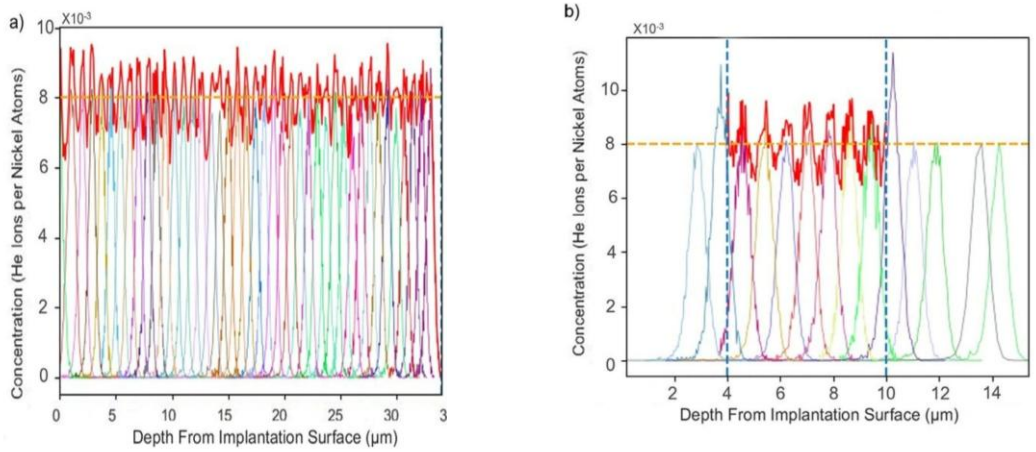

Fig. 2. (a) Helium concentration summation plot. The solid red line is the summation curve for the He concentration. (b) Helium concentration plot for the continuous area produced as the proof-of-concept experiment [15].

However, the resulting profile is not completely uniform (Fig.2), since regions with reduced impurity concentration remain throughout the entire range. An alternative method, used in the present work, is the use of a programmably rotating target, the rotation speed of which varies depending on the tilt angle according to the cotangent law [17]. As a result of this irradiation regime, an extended layer up to several micrometers thick with an almost uniform profile of the implanted impurity concentration is formed in the sample. Such a profile was demonstrated by the authors using the example of EI847 steel irradiated with helium ions [18]. This method allows the formation of a homogeneous distribution of implanted species and a more uniform defect structure. According to [18], an additional advantage of this approach is the reduced sensitivity of defect accumulation kinetics to the dose rate. As a result, the influence of the pulsed beam mode on defect evolution is significantly diminished under these conditions.

2.3. Mechanical response of irradiated materials: a nanoindentation approach

To characterize the mechanical properties of thin ion-irradiated layers, methods with high spatial resolution are needed. Nanoindentation is one of the most widely used and informative techniques for this problem [7]. The method involves the continuous penetration of a diamond indenter, typically a Berkovich tip, into the material surface while simultaneously recording the applied load (P) and indentation depth (h). This results in a load–displacement (P–h) curve, from

which key mechanical properties such as hardness (H) and elastic modulus (E) can be determined. The most commonly used analysis approach is the Oliver–Pharr method, which accounts for the indenter geometry and elastic recovery upon unloading [19].

When applying nanoindentation to irradiated materials, particular attention must be paid to size effects, including the indentation size effect (ISE) and the soft substrate effect (SSE) [20]. The ratio between the size of the plastic zone beneath the indenter and the thickness of the irradiated layer is critical. Experimental studies by Hardie et al. [8], involving transmission electron microscopy of indentation cross-sections, have shown that the shape and extent of the plastic zone depend on both indenter geometry and indentation depth. Therefore, indentation conditions must be selected such that the plastic zone remains fully within the irradiated layer.

The dispersed barrier hardening (DBH) model relates the increase in strength of irradiated materials to the presence of obstacles to dislocation motion, such as dislocation loops, voids, gas bubbles, and secondary phase particles [21]. In the present work, the increase in hardness (ΔH) is estimated based on the corresponding increase in yield strength predicted by the DBH model, using the following relationship:

$$\Delta H_i = K \cdot \alpha \cdot M \cdot \mu \cdot B \cdot \sqrt{N_i \cdot d_i} \qquad (1)$$

where:
K = 3 — conversion factor from hardness to yield strength for metals;
M — Taylor factor for FCC polycrystals M ≈ 3.06;
α — barrier strength coefficient of the obstacle;
μ — shear modulus of the matrix for austenitic steels μ = 77 GPa;
b — Burgers vector of the moving dislocation;
N_i — obstacle density (cm^{-3});
d_i — average obstacle size.

A key parameter of the DBH model is the barrier strength coefficient α, which characterizes the efficiency of a defect as an obstacle to dislocation motion. This parameter is not a universal constant and depends on several factors, including the type of defect, its size, geometry, and orientation with respect to the slip plane, as well as the deformation temperature.

The application of the DBH model to ion-irradiated materials requires consideration of several methodological aspects. These include separating the contribution of irradiation from the initial microstructure, accounting for the indentation size effect, and selecting an appropriate superposition rule for combining the contributions of different defect types [22].

For the austenitic steels considered in this work, helium bubbles can be classified as weak to intermediate obstacles. Thus, the DBH model provides a useful framework for linking microstructural features to macroscopic mechanical properties. In this study, it is used to interpret nanoindentation results by comparing experimentally measured hardening with estimates based on literature data on defect size and density.

3. Materials and Methods

Three materials were investigated in this study: two austenitic stainless steels (304L and 316L) and a high-entropy alloy (CoCrFeNiMn). Their chemical compositions are presented in Table 1.

Table 1. Chemical composition of the investigated materials.

Element	Steel 304L, wt.%	Steel 316L, wt.%	CoCrFeNiMn, at. %
C	≤ 0,03	≤ 0,03	—
Mn	≤ 2,00	≤ 2,00	20
Si	≤ 1,00	≤ 0,75	—
Cr	18,0 – 20,0	16,0 – 18,0	20
Ni	8,0 – 12,0	10,0 – 14,0	20
Mo	—	2,0 – 3,0	—
Co	—	—	20
Fe	base	base	20
P	≤ 0,045	≤ 0,045	—
S	≤ 0,030	≤ 0,030	—

Austenitic steels 304L and 316L are widely used as structural materials in nuclear power systems due to their favorable combination of mechanical strength, corrosion resistance, and manufacturability. However, under irradiation conditions, they are prone to swelling and embrittlement caused by the accumulation of radiation-induced defects and gaseous products.

As a model alternative, a CoCrFeNiMn high-entropy alloy (Cantor alloy) was considered. This alloy is one of the most extensively studied HEA systems [23]. Although it is not suitable for direct reactor applications due to neutron activation of Ni and Co, it serves as a model material for investigating radiation damage mechanisms in multi-component systems. It has been suggested that the complex chemical composition of HEAs may lead to reduced defect mobility ("sluggish diffusion"), promoting recombination of point defects and potentially enhancing radiation resistance.

The 304L and 316L steel samples were irradiated with 3 MeV He^+ and 1 MeV H^+ ions using a 5 μm thick Al degrader at the Tandetron accelerator (iThemba LABS, Cape Town, South Africa), employing the homogeneous doping method. This irradiation regime resulted in the formation of a subsurface layer with an approximately uniform distribution of implanted gases up to a depth of ~3 μm (Fig. 3).

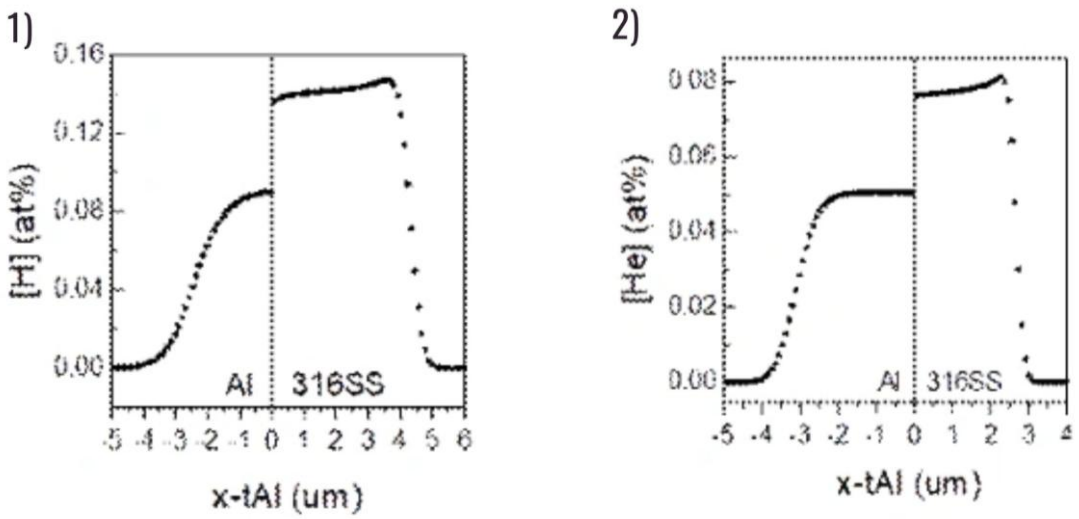

Fig. 3. Concentration profile of hydrogen (1) and helium (2) in 316L steel irradiated according to the method [1] using a 5 μm Al foil.

After irradiation, the samples were annealed at 550 °C and 650 °C for 1 hour to promote defect evolution and gas bubble growth. Nanoindentation tests

were performed using a NanoScan-4D system (TISNUM, Troitsk, Russia) with a maximum indentation depth of 500 nm. Equal loading and unloading times were used, with a holding time of 1 s at maximum load. The data were analyzed using the Oliver–Pharr method [19].

Prior to irradiation, the CoCrFeNiMn samples were subjected to standard metallographic preparation, including grinding, mechanical polishing, and final electropolishing to remove the deformed surface layer and obtain a mirror-like finish. Electropolishing was carried out using a Struers LectroPol-5 system under controlled conditions. After processing, the samples were cleaned in an ultrasonic bath to remove residual electrolyte and contaminants.

Radiation damage and implanted ion concentration profiles were calculated using the SRIM-2013 (Stopping and Range of Ions in Matter) [24], assuming a displacement energy of 40 eV.

4. Results and Discussion

The nanoindentation results are summarized in Table 2 and Fig. 5, while the corresponding values of radiation hardening (ΔH) and the estimated barrier strength coefficient (α) are presented in Table 3. The highest radiation hardening, approximately 0.8 GPa, is observed in the as-irradiated samples without post-irradiation annealing. After annealing at 550 °C, the hardening is significantly reduced to about 0.2 GPa, whereas annealing at 650 °C results in a moderate increase to ~0.3 GPa.

Since no direct microstructural characterization was performed in this study, the coefficient α in the dispersed barrier hardening (DBH) model was estimated using literature data for similar austenitic steels. According to previous studies [18], irradiation with helium up to ~0.1 at.% leads to the formation of a high density (~6.5×10^{16} cm^{-3}) of small defect clusters with sizes on the order of 1 nm. Subsequent annealing at 500 °C results in the formation of Frank dislocation loops (~6 nm, ~9.7×10^{16} cm^{-3}), while annealing at 700 °C leads to the formation of helium bubbles (~3.3 nm, ~1.7×10^{16} cm^{-3}) [17].

Table 2. Hardness (H, GPa) of 304L and 316L steels under various irradiation and annealing conditions.

Material	Ion	Annealing Temperature (°C)	Hardness (H), GPa	Standard Deviation
304L	H	-	3.45	0.26
	H	550	3.03	0.2
	H	650	2.73	0.15
	He	-	3.64	0.21
	He	550	3.03	0.20
	He	650	2.89	0.18
	He + H	-	3.93	0.16
	He + H	550	2.30	0.34
	He + H	650	2.83	0.18
316L	-	-	2.88	0.28
	-	550	2.74	0.19
	-	650	2.43	0.10
	H	-	3.70	0.00
	H	550	2.71	0.16
	H	650	3.10	0.22
	He	-	3.72	0.29
	He	550	2.94	0.22
	He	650	2.75	0.11
	He + H	-	3.12	0.33
	He + H	550	3.07	0.24
	He + H	650	2.75	0.18

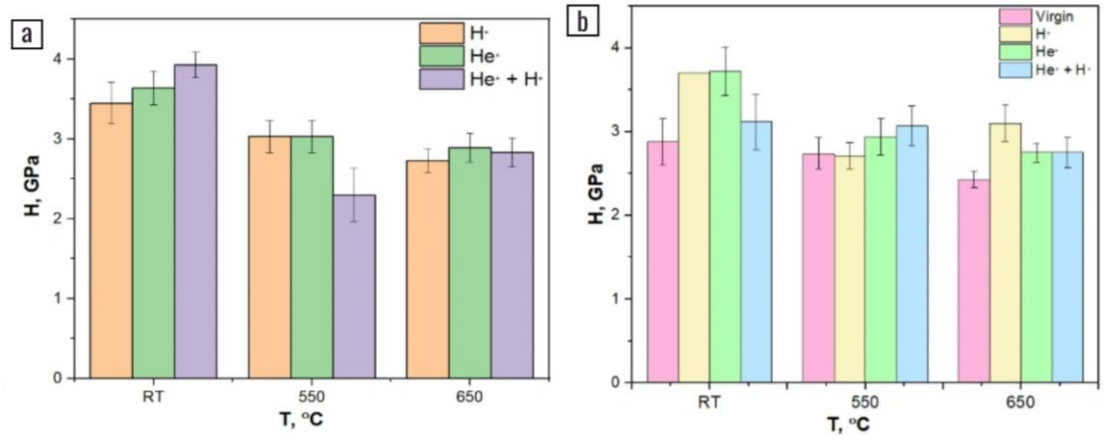

Fig. 5. Hardness (H) evolution after irradiation and subsequent annealing for (a) 304L and (b) 316L steels.

Based on these data, approximate values of α were calculated for 316L steel assuming a Burgers vector of 0.25 nm. The results are presented in Table 3. It should be emphasized that these values represent only rough estimates, as they rely on literature microstructural parameters rather than direct observations.

Table 3. Radiation hardening (ΔH) and barrier strength coefficient (α) for He^+-irradiated 316L steel based on literature data on defect microstructure.

Sample condition	ΔH, GPa	α
H	0.82	-
H, 550°C 1 h	-	-
H, 650°C 1 h	0.67	-
He	0.84	0.58
He, 550°C 1 h	0.2	0.045
He, 650°C 1 h	0.32	0.075
H+He	0.24	-
He+H, 550°C 1 h	0.33	-
He+H, 650°C 1 h	0.32	-

Despite the general expectation that larger defects act as stronger barriers to dislocation motion, the maximum hardening is observed in the as-irradiated state, where the defect size is minimal (~1 nm). This indicates that the overall hardening is governed not only by the strength of individual obstacles but also by their number density. The high density of small defect clusters in the unannealed state likely dominates the strengthening effect. It is also possible that a fraction

of these small defects remains undetected by TEM, leading to an underestimation of their actual density.

After annealing at 550 °C, radiation hardening in hydrogen-irradiated samples is not observed, which may be due to the relatively high solubility and mobility of hydrogen in the matrix. In contrast, helium stabilizes vacancy clusters, promoting the formation and persistence of defect structures. At this stage, the dominant defects are likely Frank loops, which, due to their size and character, may act as relatively weak or partially shearable obstacles to dislocation motion. Following annealing at 650 °C, the formation and growth of helium bubbles lead to an increase in the effective barrier strength, reflected in higher α values. For the samples irradiated with both helium and hydrogen, the estimated ΔH is on the order of ~0.3.

Analysis of the nanoindentation load–displacement curves, particularly the loading segments, provides indirect insight into the stress state of the near-surface layer (Fig. 4) [25]. It can be seen that for unannealed irradiated samples, the curves are significantly shifted to the right, which indicates the presence of compressive residual stresses. After annealing at 550 °C, this shift becomes less pronounced, suggesting partial stress relaxation. However, annealing at 650 °C leads to renewed stress development, likely associated with the growth of helium bubbles and the resulting volumetric effects.

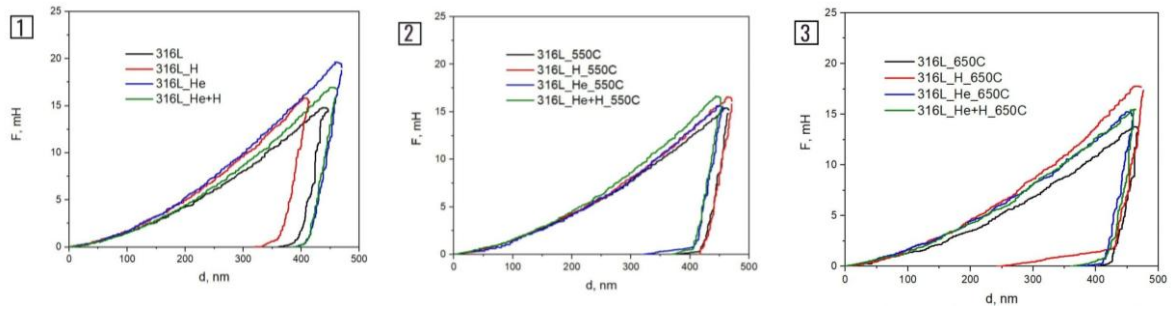

Fig. 4. Load versus indentation depth for 316L steel: (1) in the initial state; (2) after annealing at 550 °C; (3) after annealing at 650 °C.

5. Conclusion

The effect of helium and hydrogen ion implantation on the mechanical properties of austenitic stainless steels 304L and 316L has been investigated using nanoindentation. Irradiation with 3 MeV He^+ and 1 MeV H^+ ions, performed

using the homogeneous doping method, resulted in the formation of a subsurface layer with a quasi-uniform distribution of implanted gases up to several micrometers in depth.

It was shown that ion implantation leads to pronounced radiation hardening, reaching up to ~0.8 GPa in the as-irradiated state. Post-irradiation annealing at 550 °C significantly reduces the hardening, while annealing at 650 °C results in a moderate recovery of strength. This behavior is associated with the evolution of the defect structure during thermal treatment.

The results indicate that hydrogen implantation does not produce stable hardening after annealing, which can be attributed to its high mobility and solubility in the matrix. In contrast, helium stabilizes vacancy-type defects, promoting the formation of dislocation loops and gas bubbles, and thereby ensures the retention of residual hardening (~0.2–0.3 GPa).

Analysis of the nanoindentation load–displacement curves suggests the presence of compressive residual stresses in the irradiated layer. These stresses partially relax after annealing at 550 °C, while further annealing at 650 °C leads to their reappearance, likely due to helium bubble growth.

Within the framework of the dispersed barrier hardening (DBH) model, the barrier strength coefficient α was estimated using literature data on defect size and density. The highest α values (~0.8) correspond to high densities of small defect clusters in the as-irradiated state, whereas significantly lower values (~0.05) are associated with dislocation loops formed after annealing at 550 °C. At higher temperatures, the formation of helium bubbles leads to a slight increase α values (~0.07), reflecting their increased effectiveness as obstacles to dislocation motion.

The results demonstrate that the combination of the homogeneous implantation method and nanoindentation provides an effective approach for studying radiation-induced hardening in structural materials. The strong dependence of mechanical behavior on the type of implanted gas and annealing conditions highlights the importance of considering gas–defect interactions when predicting the long-term performance of materials under reactor conditions.

In addition, the pre-irradiation preparation of the CoCrFeNiMn high-entropy alloy establishes a basis for future investigations of radiation resistance in multi-component systems.

Acknowledgements

I would like to express my sincere gratitude to my research supervisor, Dr. V.A. Skuratov, for giving me the opportunity to undertake an internship at the Flerov Laboratory of Nuclear Reactions, JINR. I am grateful for his valuable advice and comprehensive support at all stages of my work. I extend my special appreciation to researcher Dr. E.A. Korneeva, Candidate of Physical and Mathematical Sciences, for her day-to-day guidance, invaluable assistance in conducting experiments, and patience as I learned the research methods. I am thankful to the administration and the members of the START team for their financial support and kindness. A special thanks to A. Zubova for her efficient handling of organizational matters, constant communication with participants, and for organizing activities that fostered professional communication, which greatly enriched my experience in the program. I express my gratitude to Al-Farabi Kazakh National University, the Faculty of Physics and Technology, and the Department of Solid State Physics and New Materials Technology for their support. I thank my thesis advisors: PhD, Research Associate G.A. Ismailova, and I.V. Danko, Deputy Head of the Department of Accelerator Technologies for Production at the Institute of Nuclear Physics of the Republic of Kazakhstan, for their mentorship and belief in me. I gained valuable knowledge, support, and the opportunity to complete my practical training at the Institute of Nuclear Physics of the Republic of Kazakhstan (Almaty) under the guidance of Dr. M.S. Merezhko, Head of the Radiation Materials Science Laboratory, for which I express my sincere gratitude. Last but not least, I thank my family and friends for their belief in me, understanding, and support, which have been a reliable foundation throughout my participation in the program.

References

[1] Fukumoto K. I. et al. Mechanical properties and microstructure in neutron-irradiated nickel-based alloys and stainless steels for supercritical water-cooled-reactor fuel cladding //Journal of Nuclear Science and Technology. – 2020. – v. 57. – №. 1. – pp. 114-120.

[2] Zinkle S. J., Was G. S. Materials challenges in nuclear energy //Acta Materialia. – 2013. – v. 61. – №. 3. – pp. 735-758.

[3] Katoh Y., Ando M., Kohyama A. Radiation and helium effects on microstructures, nano-indentation properties and deformation behavior in ferrous alloys //Journal of nuclear materials. – 2003. – v. 323. – №. 2-3. – pp. 251-262.

[4]Zinkle S. J., Snead L. L. Opportunities and limitations for ion beams in radiation effects studies: Bridging critical gaps between charged particle and neutron irradiations //Scripta Materialia. – 2018. – v. 143. – pp. 154-160.
[5]Taller S. et al. Emulation of fast reactor irradiated T91 using dual ion beam irradiation //Journal of Nuclear Materials. – 2019. – v. 527. – pp. 151831.
[6]Getto E. et al. Effect of irradiation mode on the microstructure of self-ion irradiated ferritic-martensitic alloys //Journal of Nuclear Materials. – 2015. – v. 465. – pp. 116-126.
[7] Mukhopadhyay N. K., Paufler P. Micro-and nanoindentation techniques for mechanical characterisation of materials //International materials reviews. – 2006. – v. 51. – №. 4. – pp. 209-245.
[8] Hardie, C.D., Roberts, S.G., Bushby, A.J. Understanding the effects of ion irradiation using nanoindentation techniques. Journal of Nuclear Materials, 2015, 462, 391-401.
[9] Heintze C. et al. Ion irradiation combined with nanoindentation as a screening test procedure for irradiation hardening //Journal of Nuclear Materials. – 2016. – v. 472. – pp. 196-205.
[10] Armstrong D. E. J. et al. Small-scale characterisation of irradiated nuclear materials: Part II nanoindentation and micro-cantilever testing of ion irradiated nuclear materials //Journal of Nuclear Materials. – 2015. – v. 462. – pp. 374-381.
[11] Wallace J.B., Bayu Aji L.B., Shao L., Kucheyev S.O. Radiation defect dynamics studied by pulsed ion beams // Nuclear Instruments and Methods in Physics Research Section B: Beam Interactions with Materials and Atoms. — 2017. — Vol. 409. — P. 347-350.
[12] Katoh Y., Ando M., Kohyama A. Radiation and helium effects on microstructures, nano-indentation properties and deformation behavior in ferrous alloys //Journal of nuclear materials. – 2003. – v. 323. – №. 2-3. – pp. 251-262.
[13] Trinkaus H., Singh B. N. Helium accumulation in metals during irradiation–where do we stand? //Journal of Nuclear Materials. – 2003. – v. 323. – №. 2-3. – pp. 229-242.
[14] Sohatsky, A.S., Skuratov, V.A., Janse Van Vuuren, C.A., Nguyen, V.T., O'Connell, J.H., Ibraeva, A., Zdorovets, M., Petrovich, S. Helium porosity in ODS steel containing amorphous and crystalline nanoparticles. Nuclear Instruments and Methods in Physics Research Section B, 2019, 460, 80-85.
[15] Topping M. et al. Design and implementation of an ion beam energy degrader for use in the study of nuclear materials //Journal of Nuclear Materials. – 2023. – v. 573. – pp. 154099.
[16] Gasparrini C. et al. Micromechanical testing of unirradiated and helium ion irradiated SA508 reactor pressure vessel steels: Nanoindentation vs in-situ microtensile testing //Materials Science and Engineering: A. – 2020. – v. 796. – pp. 139942.
[17] Sohatsky, A.S., Komarova, D.A., Nguyen, T.V., Skuratov, V.A., Mitrofanov, S.V., Khumalo, Z.M., Mtshali, C., Nkosi, M., O'Connell, J.H. Novel methodology of homogeneous ion doping/damage of nuclear materials for structural characterization. Journal of Nuclear Materials, 2025, 606, 155601.
[18] Nguyen Van Tiep, E.A. Korneeva, A.S. Sokhatsky, V.A. Skuratov, S.V. Mitrofanov, D.A. Komarova, M. Nkosi. Structure and properties of austenitic alloys irradiated with helium at appm He/dpa > 1000 // The Sixteenth International Ural Seminar on Radiation Damage Physics of Metals and Alloys, 2 – 6 March. - Sysert, Russia. 2026 – p. 34.

[19] Oliver W. C., Pharr G. M. An improved technique for determining hardness and elastic modulus using load and displacement sensing indentation experiments //Journal of materials research. – 1992. – v. 7. – №. 6. – pp. 1564-1583.
[20]Kasada R. et al. A new approach to evaluate irradiation hardening of ion-irradiated ferritic alloys by nano-indentation techniques //Fusion engineering and design. – 2011. – v. 86. – №. 9-11. – pp. 2658-2661.
[21] Bergner F. et al. Application of a three-feature dispersed-barrier hardening model to neutron-irradiated Fe–Cr model alloys //Journal of Nuclear Materials. – 2014. – v. 448. – №. 1-3. – pp. 96-102.
[22] Lai L., Brandenburg J.E., Chekhonin P. et al. Microstructure-informed prediction of hardening in ion-irradiated reactor pressure vessel steels // Metals. — 2024. — Vol. 14(3). — 257. DOI: 10.3390/met14030257.
[23] Barron, P., Carruthers, A.W., Middleburgh, S., Armstrong, D., Gandy, A., Pickering, E.J. High-Entropy Alloys for Advanced Nuclear Applications. Entropy, 2021, 23, 98.
[24] Ziegler, J.F., Ziegler, M.D., Biersack, J.P. SRIM – The stopping and range of ions in matter (2010). Nuclear Instruments and Methods in Physics Research B, 268, 1818–1823.
[25] Zhu L. N. et al. Measurement of residual stresses using nanoindentation method //Critical Reviews in Solid State and Materials Sciences. – 2015. – v. 40. – №. 2. – pp. 77-89.